

Treatment of Surface Emissivity for Satellite Microwave Data Assimilation

Fatima Karbou

*CNRM / GAME, MÉTÉO-FRANCE & CNRS
Toulouse, France
fatima.karbou@meteo.fr*

SUMMARY

Observations from satellite microwave instruments have a large information content and are known to improve the quality of global analyses of the atmosphere. However, the use of these observations remains far from being optimal. Indeed, only microwave observations, for which the surface contribute the least, are currently assimilated. This restriction is mainly due to remaining uncertainties about the surface emissivity and the skin temperature. For many reasons, uncertainties about the surface have a larger impact over land than over ocean. Recent assimilation experiments have been conducted in order to assimilate more microwave observations over land. To do so, different methods have been used in order to estimate the land emissivity and/or the land skin temperature directly from satellite observations. This paper describes the methods used to estimate the land emissivity and the skin temperature within the constraints of variational assimilation systems. An overview of the assimilation experiments conducted in many NWP centres is also given together with their main results.

KEYWORDS: Land surface emissivity Microwave observations over land Low orbiting satellites Data assimilation systems

1 Introduction

Microwave instruments from low orbiting satellites provide relevant observations which improve the initial conditions for short-range forecasts. Nevertheless and in spite of their information content, these observations are far from being optimally used in Numerical Weather Prediction (NWP). One important concern to be addressed about the use of satellite microwave observations is that they are not as intensively used over land as they are over sea. Only channels that are weakly sensitive to the land surface are used. The uncertainties about the surface are more critical over land than over ocean. In fact, (1) sea emissivities are low, generally close to 0.5, whereas land emissivities are rather close to 1.0. Consequently, the surface contribution to the measured signal is less important over sea than over land. Moreover, (2) many authors have explored the sea emissivity modeling issues and have provided emissivity models with proven effectiveness (Deblonde and English 2000; Guillou *et al.* 1998; Prigent and Abba 1990; Guissard and Sobieski 1987; Wentz 1975; Rosenkranz and Staelin 1972). The FASTEM-3 sea emissivity model (English and Hewison, 1998, Deblonde 2000) is used in many NWP centres including the Met-Office, ECMWF and MÉTÉO-FRANCE. FASTEM-3 is a fast Geometric Optics (GO) model that includes parametrizations of the dielectric sea water, the surface roughness and the foam. NCEP uses two options to model the sea emissivity: the use of FASTEM (operational) or the use of the NESDIS two-scale Ocean Model (Weng and Liu, 2003). The performances of sea emissivity models are good enough to meet the NWP requirements although there are still some well identified problems. Indeed, a perfect sea emissivity model, if it existed, would hardly compensate for the errors in the model's input parameters. Moreover, GO models are known to work better at high frequencies than in the low frequency range. In order to improve the sea emissivity modeling at low frequencies, a new sea emissivity model (called low frequency model) has been developed (Kazumori *et al.* 2007). This low frequency model contains an empirical two scale roughness

parametrization and uses coefficients derived from the fitting to satellite measurements. This model has been compared with the FASTEM and the NESDIS ones and has shown a potential to improve the brightness temperature biases (observations-simulations) at frequencies lower than 20 GHz.

Unlike sea emissivities, microwave land surface emissivities are rather high (almost 1.0) and vary in a complex way with surface types, roughness and moisture among other parameters. Being important and variable, the land surface contribution to the measured radiance could not be separated from the atmosphere contribution unless the surface is accurately described. English (1999) has shown that emissivities determined with an accuracy better than 2% could be used for sounding channels to reduce humidity profile retrieval errors over land. However, the extend to which microwave window and sounding channels could be better used over land depends not only on the land emissivity but also on the land skin temperature (English, 2007). A land emissivity climatology combined with accurate skin temperatures have been found useful to retrieve atmospheric temperature and humidity information over land from AMSU-A & AMSU-B measurements (Karbou *et al.* 2005b).

As pointed out earlier, a good knowledge of the surface, in both emissivity and skin temperature, is crucial for a better use of satellite microwave observations. In the past decades, many studies either on the estimation or on the modeling of the land surface emissivity have been published. Tremendous efforts have been expended to improve our knowledge about the emission of land surfaces. Useful information have been further gained toward physical parametrizations together with direct or indirect measurements of the land emissivities. Many studies have provided useful land emissivity models despite their uncertainties (Grody (1988), Isaacs *et al.* (1989), Weng *et al.* (2001)). The emissivity model's uncertainties essentially come from the lack of input parameters that are necessary to feed most of the models. Besides the modeling approaches, land emissivities have been estimated from *in-situ* measurements (Calvet *et al.* (1995), Matzler (1994, 1990), Wigneron *et al.* (1997) among others), airborne measurements (Hewison and English (1999), Hewison (2001)) and satellite observations (Choudhury (1993), Felde and Pickle (1995), Jones and Vonder Haar (1997), Karbou *et al.* (2005), Morland *et al.* (2000, 2001), Prigent *et al.* (1997), among others).

Most NWP models use the empirical formulations of Grody (1988) and Weng *et al.* (2001) models to determine the land emissivity at microwave frequencies. Such methodologies make it possible to assimilate microwave observations from channels weakly sensitive to the land surface. However, the concern about the assimilation of surface sensitive channels can not be addressed using these models. Alternatives to emissivity models have been recently proposed to help the assimilation of surface sensitive microwave observations. The main objective of this paper is to describe recently developed methodologies, as alternatives to empirical models, to better characterize the land surface. A particular attention is paid to the effectiveness of these methods within the constraints of data assimilation systems.

The paper is organized as follows: section 2 presents the methodologies used to estimate the land emissivity from satellite observations. A particular attention is paid to describe sources of errors that are the most dominant for the land emissivity. The emissivity variability is also discussed. An overview of recent assimilation experiments to help assimilating more microwave observations over land is given in section 3. The experiment results are also evaluated in this section. Section 4 gives a summary and draws some conclusions.

2 Land emissivity retrieval from satellite observations

2.1 Satellite microwave measurements

Observations from The advanced microwave sounding unit (AMSU) -A and AMSU-B, the Special Sensor Microwave Imager (SSM/I), the Special Sensor Microwave Imager/Sounder (SSMIS), the Advanced Microwave

Scanning Radiometer - Earth Observing System (AMSR-E), the tropical Rainfall Measurement Mission Microwave Imager (TRMM) Microwave Imager (TMI) among other instruments are increasingly used in NWP models.

AMSU-A & -B are on board the latest generation of the National Oceanic and Atmospheric Administration (NOAA) polar orbiting satellites since May 1998. Moreover, the National Aeronautics and Space Administration (NASA) Aqua mission and more recently the Metop-A mission carried similar instruments (MHS for AMSU-B). These instruments measure the outgoing radiance from the atmosphere and the Earth surface. AMSU-A, that has many channels close to the oxygen absorption band, is designed to provide the atmospheric temperature at many levels from about 45 km down to the Earth surface. AMSU-B makes measurements near the water vapour absorption line at 183.31 GHz in order to provide the atmospheric humidity. In addition to sounding channels, AMSU-A and AMSU-B have, the so called “window channels”, that are mainly sensitive to the surface and to the low atmosphere layers (23.8, 31.4, 50.3, 89, and 150 GHz). Both instruments sample 30 and 90 Earth views with a nominal field of view of 3.3° and 1.1° respectively. The AMSU observation scan angle varies from -48° to $+48^\circ$ which translates into $\pm 58^\circ$ zenith angle variation.

The SSM/I is a conical scanning passive microwave imager and is on-board the latest generation of the DMSP satellites since June 1987. SSM/I observations are made at four frequencies (19.3, 22.2, 37.0 and 85.5 GHz), with a dual polarization (only horizontal at 22.2 GHz) and at a near constant zenith angle of 53° . SSM/I observations have been intensively used to determine the sea wind speed, the integrated water vapour, the cloud liquid water, etc.

The Defense Meteorological Satellite Program (DMSP) F-16, F-17 satellites carry the first generation of Special Sensor Microwave Imager/Sounder (SSM/I-S). This sensor provides, for the first time, observations of the atmospheric temperature and humidity using a conical scanning technique. SSM/I-S has 14 channels in the 50-60 GHz range which allow atmospheric temperature sensing from about 80 km down to the earth surface. In addition to temperature sounding channels, SSM/I-S combines humidity sounding channels close to the strong 183 GHz water vapour line as well as imaging channels shared with SSM/I.

The AMSR-E is operating aboard NASA's Aqua Satellite since 4 May 2002. It is a twelve-channel, six-frequency, passive-microwave radiometer system with a near constant zenith angle of about 55° . It measures horizontally and vertically polarized brightness temperatures at 6.9, 10.7, 18.7, 23.8, 36.5, and 89.0 GHz.

The TMI instrument is aboard the TRMM mission since November 1997 and measures the intensity of radiation at five separate frequencies: 10.7, 19.4, 21.3, 37, 85.5 GHz. The TRMM orbit altitude is close to 400 km. As a consequence, TMI has a 760 km wide swath width with a high and variable horizontal resolution (from 6 km at 85.5 GHz to 50 km at 10.7 GHz) and also with an observation zenith angle ranging from about 47° to 53° .

2.2 Land emissivity calculation

Assumptions commonly adopted to calculate the land emissivities from satellite observations are that the surface temperature and the skin temperature are the same, that there is no volume scattering and that the surface, supposed to be flat, has a specular reflection (Jones and Vanderhaar 1997; Prigent *et al.* 1997; Weng *et al.* 2001; Karbou *et al.* 2005a among others). The last assumption has been adopted since no *a priori* information about the surface are available. The use of this assumption for nadir viewing instruments, like AMSU-A & AMSU-B, is questionable for specific cases (Mätzler 2005). The author recommends the use of a specular parameter, to be determined over the globe. Karbou and Prigent (2005) have shown that the impact of the specular assumption on the retrieved near-nadir AMSU emissivities when the surface is lambertian, is well below 1% of emissivity bias over natural snow-free areas. Nevertheless, the use of a specular parameter, when available at a global scale, should correct the effect of the surface assumption. This should be beneficial over,

at least, snow surfaces involved with volume scattering.

For a non-scattering plane-parallel atmosphere and for a given instrument path zenith angle and frequency, the brightness temperatures (noted T_b , hereafter) observed by the sensor can be expressed as:

$$T_b(\nu, \theta) = T_s \varepsilon(\nu, \theta) \Gamma + (1 - \varepsilon(\nu, \theta)) \Gamma T_a^\downarrow(\nu, \theta) + T_a^\uparrow(\nu, \theta) \quad (1)$$

$$\Gamma = \exp\left(\frac{-\tau(0, H)}{\cos(\theta)}\right) \quad (2)$$

where $T_b(\nu, \theta)$ and $\varepsilon(\nu, \theta)$ represent the T_b measured by the sensor and the surface emissivity at frequency ν and at observation zenith angle θ respectively. T_s , $T_a^\downarrow(\nu, \theta)$, and $T_a^\uparrow(\nu, \theta)$ are the skin temperature, the atmospheric down-welling and upwelling T_b s respectively. Γ is the net atmospheric transmissivity and can be expressed as a function of the atmospheric opacity $\tau(0, H)$ and the observation zenith angle θ . H is the top of atmosphere height.

The microwave land emissivity can then be retrieved as follows.

$$\varepsilon(\nu, \theta) = \frac{T_b(\nu, \theta) - T_a^\uparrow(\nu, \theta) - T_a^\downarrow(\nu, \theta) \Gamma}{(T_s - T_a^\downarrow(\nu, \theta)) \Gamma} \quad (3)$$

AMSU measurements are made with a system of rotating antennae. As a consequence, the calculated emissivities are a mixture between emissivities in the vertical and the horizontal polarisations. Under the assumption of a nominal performance of the AMSU instrument, this relationship could be expressed by:

$$\varepsilon(\nu, \theta) = \varepsilon_p(\nu, \theta) \cos^2(\varphi) + \varepsilon_q(\nu, \theta) \sin^2(\varphi) \quad (4)$$

$$\varphi = \arcsin\left(\frac{R}{R + H_{sat}} \sin(\theta)\right) \quad (5)$$

Here, θ and φ are the satellite zenith and scan angles respectively. φ can be expressed as a function of the observation zenith angle θ , the radius of the Earth R and the satellite height H_{sat} .

$\varepsilon_p(\nu, \theta)$ and $\varepsilon_q(\nu, \theta)$ are emissivities at the two orthogonal polarisations. For AMSU window channels, the polarisation is assumed to be vertical at nadir. Consequently, equation (3) translates into:

$$\varepsilon(\nu, \theta) = \varepsilon_v(\nu, \theta) \cos^2(\varphi) + \varepsilon_h(\nu, \theta) \sin^2(\varphi) \quad (6)$$

Here, $\varepsilon_v(\nu, \theta)$ and $\varepsilon_h(\nu, \theta)$ are emissivities at the vertical and horizontal polarisations respectively.

2.3 Land emissivity analysis

Land emissivities derived from satellite observations are in fact "averaged emissivities" integrated over the instrument field of view. For evaluation purposes, it is highly desirable that the satellite emissivities can be compared with in-situ emissivity measurements. However, such measurements are sadly missing at global scale. Therefore, alternatives have to be used to evaluate satellite data based emissivity estimates.

1. One possible approach is to examine how the land emissivity compensates for errors in the input parameters. From Equ. (3), one can see that emissivity errors are mostly determined by errors coming from

the skin temperature, the observed T_b , the humidity and temperature profiles and more generally from the radiative transfer modeling. The emissivity change induced by a variation in one input parameter can be examined and can indicate the most dominant sources of error. The emissivity sensitivity to errors in the input parameters have been previously studied using data from AMSU-A & AMSU-B (Karbou *et al.* 2005a). In this study, the impacts of an alteration of $\pm 15\%$ in the humidity profile, ± 1 K in the temperature profile, ± 4 K in the skin temperature, and ± 1 K in the brightness temperature have been examined. It was found that, for all AMSU channels, emissivity errors are larger for high zenith angles and for very moist conditions. Indeed, the sensitivity to the surface decreases with decreasing atmospheric transmission. The latter decreases with increasing zenith angle and with increasing total water vapour. Errors in the humidity profiles are found to have non negligible effects at 89 and at 150 GHz and a less important effect on the surface channels 23.8, 31.4 and 50.3 GHz (less than 0.25% of relative error). Errors in skin temperatures have a large impact on the estimated emissivity at all frequencies (up to 3% of emissivity relative errors). As expected, errors in the air temperature profile produce larger emissivity variations at 50 GHz than at other frequencies located far from the oxygen absorption bands.

2. Besides the emissivity sources of error analysis, the consistency of the retrieved emissivities can be checked. The analysis of the emissivity variability, at least, in space, in frequency, in polarization and in observation angle can provide valuable information to illustrate the complex mechanisms behind the land surface emission. Moreover, inter-sensor emissivity comparison can tell the consistency of the emissivities and the inter-calibration of the instruments. Microwave land emissivities have been calculated following the methodology described in section 2.b within the M  T  O-FRANCE and the ECMWF 4D-var assimilation systems (Karbou *et al.* 2006-2007). The atmospheric components have been computed using the RTTOV model (Eyre 1991; Saunders *et al.* 1999; Matricardi *et al.* 2004). Atmospheric temperature and humidity profiles as well as surface temperature have been taken from the model's short-range forecasts. The cloud clearing has not been optimal since an *a priori* knowledge of cloud contamination is difficult to obtain in the constraints of assimilation systems. Emissivities have been calculated for many microwave channels coming from different microwave sensors (AMSU-A, AMSU-B, SSM/I, SSMI/S, TMI and AMSR-E). Mean emissivity map averaged using AMSU-A channel 3 (50.3 GHz) emissivity estimates from March 2007 and mean emissivity difference map between vertical (V) and horizontal (H) polarizations at 19 GHz from SSM/I channels 1&2 from November 2006 are shown in Figure 1 and Figure 2 respectively. In general, emissivity averaged maps show expected spatial variation of the emissivity. Bare soils are associated with lower emissivities and a high emissivity polarization difference. Emissivities for forests are high and have a small variation with the polarization. Emissivities for lakes and rivers are rather low and highly variable. Water has high dielectric values that translate into low emissivities. Moreover, the lakes emissivity variability is probably related to the change in the percentage of (land, water) for each pixel between satellite overpassings. Over snow, the emissivity has larger standard deviations. Indeed, snow emissivities depends on the physical properties of snow with a strong contrast between wet & dry snow. Emissivities are believed to decrease with increasing frequency over dry snow (Matzler, 1994).

The emissivity retrieved from cross-track instruments varies with respect to the observation zenith angle. A strong and a negligible dependencies of the AMSU emissivity with the zenith angles over bare soils and over dense vegetation areas, respectively, have been noticed (Karbou *et al.* 2005a). A rather good agreement between emissivities from many sensors has been observed (Karbou *et al.* 2007). For most surface types, the emissivities have been found to vary smoothly in frequency (Choudhury (1993), Jones and Vonder Haar (1997), Karbou *et al.* (2005a), Prigent *et al.* (2000)). It has been shown that it is possible to describe the emissivity angular and spectral variations with polynomial best-fit functions that could be used to model the land emissivity at AMSU frequencies (Karbou 2005). Another important assumption is that, for cross-track instrument like AMSU-A & AMSU-B, emissivities retrieved from "window" channels could be used as a "good approximation" for sounding channels (Karbou *et al.* (2005a-2005b)).

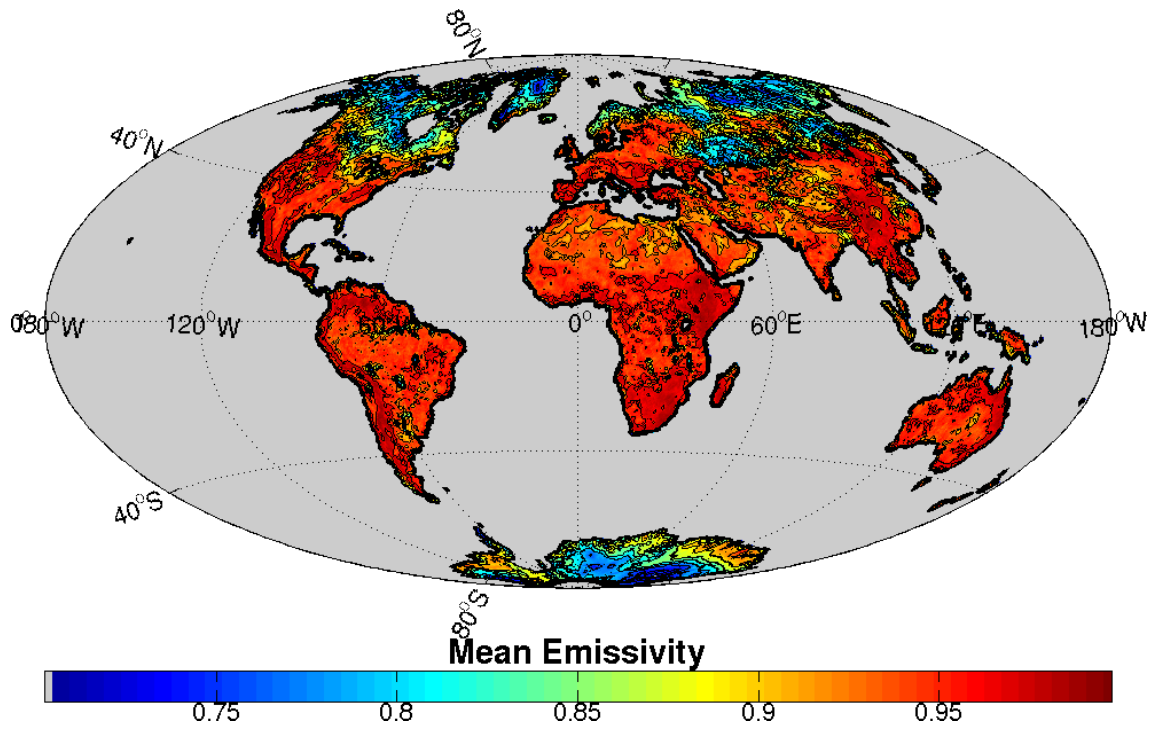


Fig. 1: Mean emissivity map at 50.3 GHz (AMSU-A channel 3) averaged over one month (March 2007).

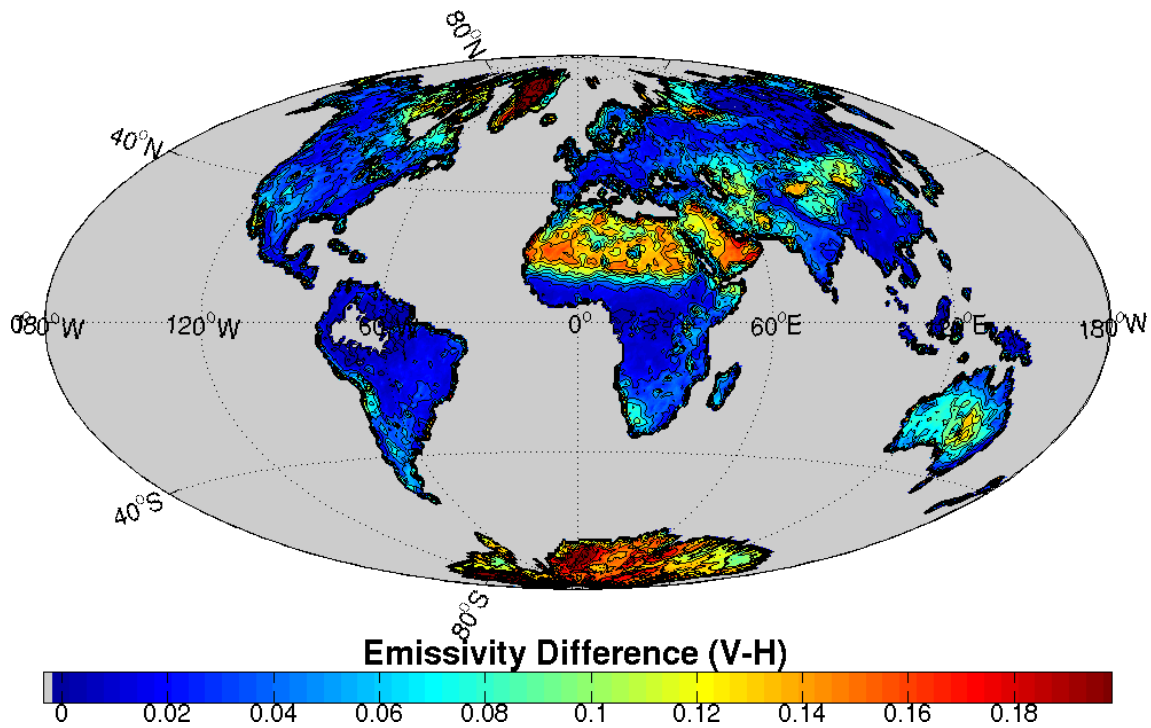


Fig. 2: Emissivity polarization difference map at 19 GHz (V-H) and obtained using one month of SSM/I observations (November 2006).

3 Land emissivity and skin temperature for data assimilation

3.1 Overview

NWP have privileged the use of variational methods to assimilate satellite observations. These methods seek for a model state that verifies the optimal balance between the background constraints and all available observations. However, many issues are still to be addressed to fully benefit from satellite observations. Only few studies have addressed the issue of land affected observation assimilation by exploring different ways to constrain the land emissivity and/or the skin temperature. 1D-Var based sensitivity studies have been performed at the Met-Office using simulated observations at AMSU-A sounding frequencies. It has been found that the performances of the 1D-Var are best when the surface emissivity is not taken constant but is described using an emissivity climatology previously derived using observations from AMSU-A window channels (from Karbou *et al.* 2006). Further studies are underway to examine the impact of land emissivity climatologies in the framework of the Met-Office assimilation system and to improve the analysis of the land skin temperature. Other studies have been undertaken at MÉTÉO-FRANCE and at ECMWF and will be described in the next sections.

3.2 Experiments at MÉTÉO-FRANCE

Recent studies have been performed at MÉTÉO-FRANCE in order to find strategies, effective enough, to assimilate surface affected microwave observations. In this context, properties highlighted by previous land emissivity analysis studies have been essential. In particular, the following assumptions have been adopted. For most surface types, the land emissivity varies smoothly in frequency and that for cross-track instruments, like AMSU-A & AMSU-B, emissivities retrieved from “window” channels could be used as a “good approximation” for sounding channels. Three methods have been tested in order to study the relevance of using land emissivity and/or skin temperature, directly calculated from satellite observations, to improve the assimilation of surface affected observations (Karbou *et al.* 2006). These methods, with increasing complexity, have been interfaced with the RTTOV model and have been first applied to AMSU-A and AMSU-B measurements.

1. The first method (called method1 hereafter) is based on the use of averaged emissivities previously estimated over 2 weeks prior to the assimilation period using observations from AMSU window channels (23.8, 31.4, 50.3 and 89 GHz). Emissivities for sounding channels are taken from their estimates at the closest (in frequency) window channels. For example, averaged emissivities at 50 GHz (AMSU-A channel 3) and at 89 GHz (AMSU-B channel 1) are given to AMSU-A temperature sounding channels and to AMSU-B humidity sounding channels respectively. When using this method during the assimilation, the skin temperature is taken from the model’s short-range forecasts. A first assimilation experiment (called EXP1) has been run applying this method to AMSU-A and AMSU-B observations.
2. The second method (called method2 hereafter) uses a dynamically varying emissivities derived at each pixel using only one channel per instrument. The dynamically estimated emissivity is then given to the remaining channels without any frequency parametrization. When using this method during the assimilation, the skin temperature is taken from the model’s short-range forecasts. A second assimilation experiment (called EXP2) has been run applying this method to AMSU-A and AMSU-B observations. Emissivities dynamically derived at 23.8 GHz (AMSU-A channel 1) and at 89 GHz (AMSU-B channel 1) are given to the remaining AMSU-A and AMSU-B channels respectively.
3. And finally the third method (called method3 hereafter) combines the two previous ones. It uses averaged emissivities and dynamically estimated skin temperature at each pixel using one window channel of each instrument. The estimated skin temperature replaces the surface temperature coming from the model’s

short range forecasts. At a selected frequency ν_1 , the skin temperature can be derived from equation (1) as follows.

$$T_s = \frac{T_b(\nu_1, \theta) - (1 - \epsilon_{atlas}) T_a^\downarrow(\nu_1, \theta) \Gamma - T_a^\uparrow(\nu_1, \theta)}{\epsilon_{atlas} \Gamma} \quad (7)$$

Here, T_s , $T_b(\nu_1, \theta)$, $T_a^\uparrow(\nu_1, \theta)$, $T_a^\downarrow(\nu_1, \theta)$, and Γ are the skin temperature, the observed T_b , the atmospheric upwelling and downwelling T_b s and the net atmospheric transmission at frequency ν_1 and observation zenith angle θ respectively. ϵ_{atlas} represents mean emissivity atlas averaged over at least two weeks. It should be mentioned that the land emissivity climatology should be as unbiased as possible to avoid error propagation into skin temperature estimates. A third assimilation experiment (called EXP3) has been run applying this method to AMSU-A and AMSU-B observations. Averaged emissivities derived at 50 GHz (AMSU-A channel 3) and at 89 GHz (AMSU-B channel 1) have been given to AMSU-A temperature sounding channels and to AMSU-B humidity sounding channels respectively. The dynamically estimated skin temperature at AMSU-A channel 1 (23.8 GHz) has replaced the skin temperature coming from the model's short-range forecasts.

The performances of the three land methods have been studied in terms of T_b departures (observation-simulation) from first guess (called fg-departures hereafter) and also in terms of analysis and forecast impacts. The operational model has been used as a reference for the assimilation experiments. The four experiments have been run over different periods in years 2005 and 2006. It has been found that all new land methods are effective in bringing AMSU simulations closer to the observations. Figure 3 shows the fg-departure histograms obtained from 4 experiments: the control and experiments using land methods 1 to 3 respectively. The histograms are for a two week period (late August 2005) and are shown for AMSU-A channel 3 (50.3 GHz), AMSU-A channel 15 (89 GHz) and AMSU-B channel 2 (150 GHz). The best results are obtained using the second and the third methods. It should be noted that not only window channels benefit from the land emissivity but also sounding channels. (i) The experiments use a check on the fg-departures of the window channels 4 for AMSU-A (absolute departures should be below 0.7 K) and of channel 2 for AMSU-B/MHS (absolute departures should be below 5.0 K) to identify data with a too strong cloud contamination for the lower-peaking channels. If these tests are successful then data from sounding channels are accepted during the assimilation. (ii) Figure 4 shows daily time series (July 2005) of fg-departure RMS of errors calculated from AMSU-A surface (subplots (a), (b) and (f)) and sounding channels (subplots (c), (d), and (e)) and obtained from the control (in black) and from experiment 2 (in blue). One should notice that RMS errors are significantly reduced with experiment 2 for both surface and sounding channels.

The improvement of the observation operator simulations is associated with a significant increase in the number of observations that could be assimilated over land. With respect to the control, methods 2 and 3 have induced an increase of up to 140% in the number of AMSU-B channel 2 (150 GHz) observations that pass the quality control check. Other assimilation experiments over longer periods have run assimilating different combination of AMSU channels. The land methods have been also extended to use SSM/I observations over land. The forecast scores have been found to be generally neutral to positive for temperature, humidity and geopotential height.

Nevertheless, this work is far from being completed since efforts are still needed to better assess the impact of each land method on the analysis and on the forecasts. This could not be done since the important issues of bias correction and cloud identification are carefully addressed. Further work is underway to improve the land emissivity methods and to carefully select microwave channels candidate to be assimilated over land.

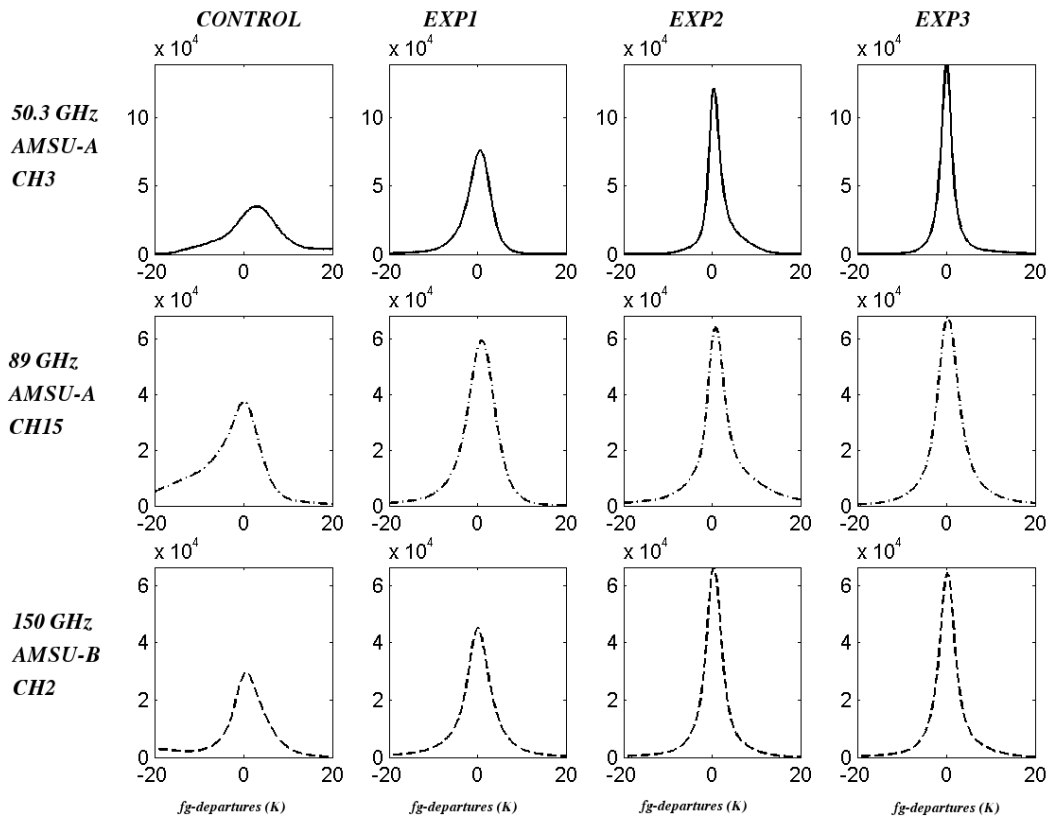


Fig. 3: 2 week period (late August 2005) fg-departure histograms obtained from 4 experiments: the control and experiments using land emissivity methods 1 to 3 respectively. The histograms are shown for AMSU-A channel 3 (50.3 GHz), AMSU-A channel 15 (89 GHz) and AMSU-B channel 2 (150 GHz) (from Karbou et al. 2006).

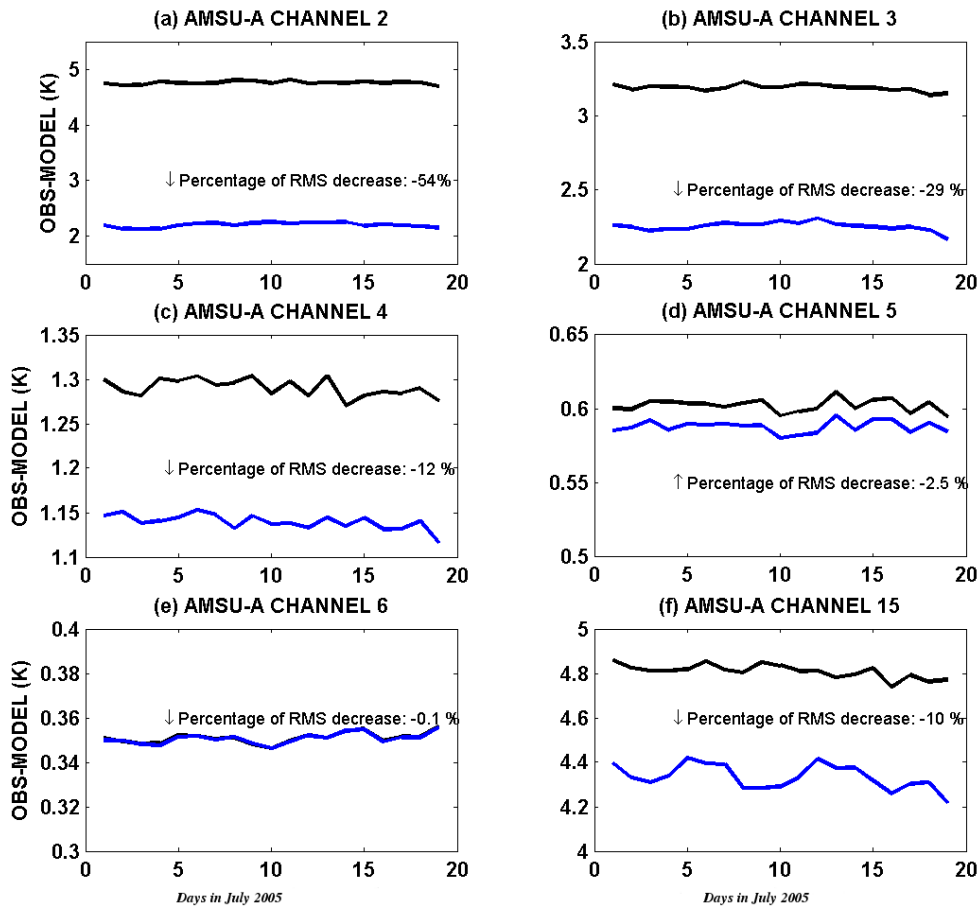


Fig. 4: Time series (July 2005) of fg-departure RMS of errors calculated from AMSU-A surface (subplots (a), (b) and (f)) and sounding channels (subplots (c), (d), and (e)) and obtained from the control (in black) and from experiment 2 (in blue) (from Karbou et al. 2006).

3.3 Experiments at ECMWF

Studies have been conducted at ECMWF with the aim to improve the assimilation of microwave observations that receive a contribution from the land surface. Direct calculation of land emissivities from AMSU-A measurements have been done at ECMWF (Prigent *et al.* (2005). These estimates have been compared with emissivities extrapolated from SSM/I ones and with emissivities coming from empirical models.

Activities have been also initiated towards the assimilation of microwave observations over land under cloudy and rainy situations (O'Dell and Bauer, 2007). Such developments are believed to better constrain the moisture analysis and then to improve the precipitation forecasts over land. A two-step method (1D+4D-Var) has been used at ECMWF to assimilate cloudy SSM/I sea observations since June 2005 (Bauer *et al.* 2006a-2006b). Cloudy SSM/I radiances are first assimilated within the 1D-Var to produce Total Column Water Vapour (TCWV). Then, TCWV are given to 4D-VAR as "pseudo-observations". This approach has been adapted for the assimilation, in a similar way, of cloudy SSMI/S radiances in land situations. Monthly derived SSM/I emissivities (Prigent *et al.* 2006) have been used to construct a true background climatology of emissivity and to define appropriate emissivity background errors. Prior to the assimilation experiments, sensitivity studies have been conducted in order to measure the response of SSMI/S channels to clouds over sea and over land. Figure 5 shows the theoretical change in TB induced by a change in rain water path (RWP) of 0.1 kg/m² for both sea (blue circles) and land profiles (black squares). The results are given for a selection of SSMI/S channels. It has been found that, information about clouds is more difficult to obtain over land than over ocean. For instance, Figure 5 shows that measurements close to 19, 37, 50 GHz seem to have no sensitivity to rainfall over land. In the other hand, measurements close to 91 and 150 GHz show acceptable sensitivity to clouds over land. According to the sensitivity study results, many assimilation experiments have been run with SSMI/S channels that have the larger sensitivity to clouds over land. It has been shown that the 1D-Var system seems to be working as desired for precipitating regions. Nevertheless, drying humidity increments were generally allowed into the 4D-Var system while the moistening increments were penalized. This result is consistent with previous findings using cloudy SSM/I observation assimilation over sea. Based on the described initial results, research studies will be pursued with the aim to ultimately assimilate cloudy observations directly in the 4D-Var.

Following the methodologies developed at MÉTÉO-FRANCE for the assimilation of surface sensitive observations (Karbou *et al.* 2006), three methods have been implemented in the ECMWF 4D-Var assimilation system. The methods, initially developed for AMSU-A, AMSU-B and SSM/I, have been extended to treat observations from SSMI/S, TMI and AMSR-E (Karbou *et al.* 2007).

Using these methods, a first set of assimilation experiments has been run using temperature sounding channels from SSMI/S observations. The control experiment assimilates SSMI/S temperature channels over sea. A second experiment (called experiment-dyn) that assimilates SSMI/S temperature sounding channels over sea and land has been run. For this experiment, emissivities dynamically derived at 50H, 19V, 91H have been used (method 2). Temperature sounding channels receive the 50H emissivity whereas the remaining channels (not assimilated but monitored) receive the 19 V or H emissivities. A third experiment (called 'experiment-skin' hereafter) that assimilates SSMI/S temperature sounding channels over sea and over land has been also carried out. For this experiment, an emissivity climatology, calculated using two weeks of data prior to the assimilation period, has been used. Moreover, the skin temperature has been estimated for each pixel at 19V (method 3) and has replaced the skin temperature coming from the model's short-range forecasts. Overall, no divergence between the assimilation of SSMI/S observations over land and the assimilation of other observations has been noted. Indeed, the fit of other observations against the First Guess or the analysis is not altered when SSMI/S temperature observations are assimilated over land for both experiment-dyn and experiment-skin. Figure 6 shows the statistics for the FG (solid) and the analysis departures (dashed) for the assimilated SSMI/S observations within the control (red) and the experiment-dyn (black). Results are given in terms of standard deviations, biases and number of assimilated observations. For SSMI/S observations, adding channels 2, 3, and 4 (52.8

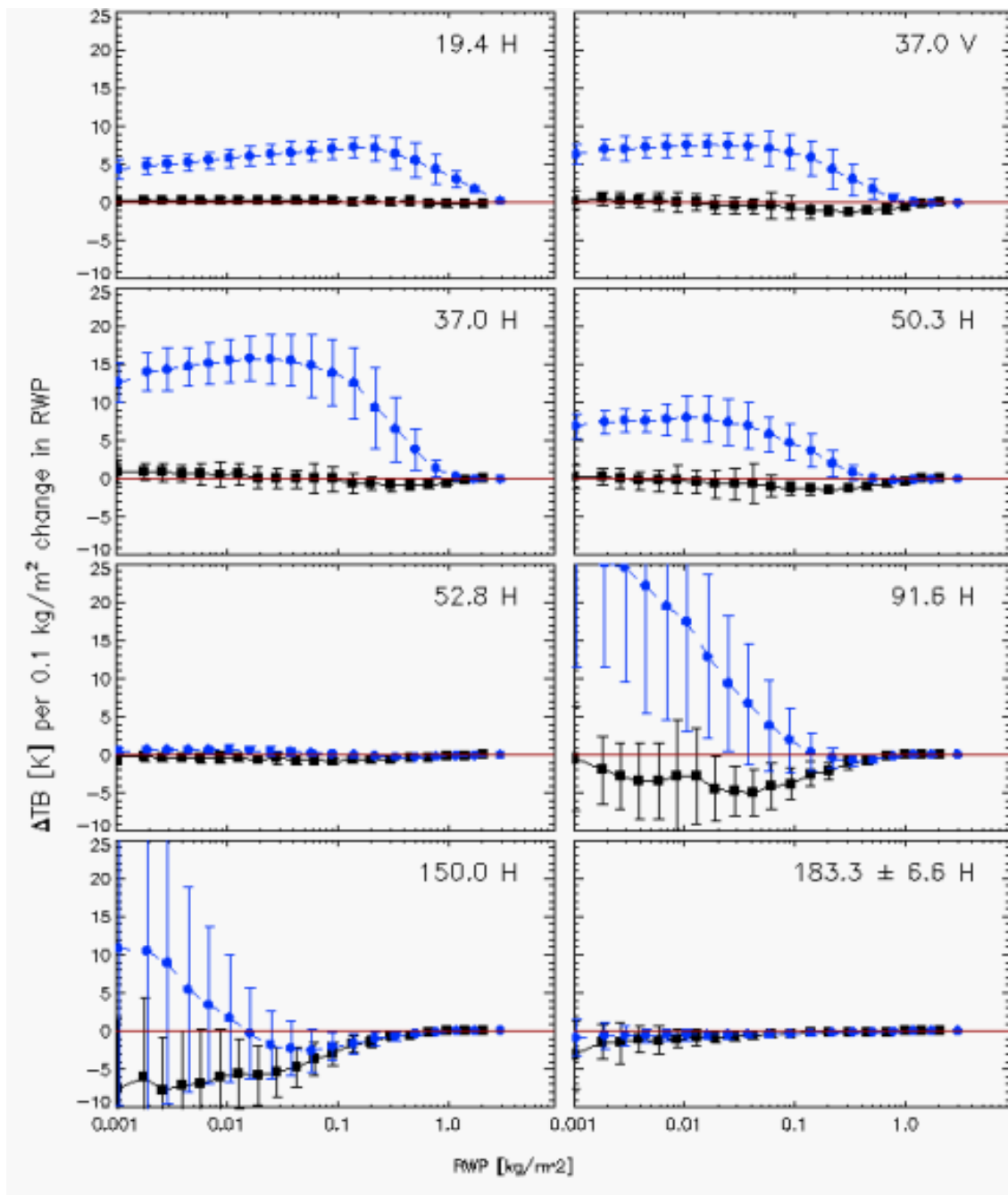


Fig. 5: The main change in TB for selected SSMIS channels to a 0.1 kg/m² change in rain water path (RWP), distributed in proportion to the existing rain profile; 20,000 random profiles from a single model run at T799 resolution were used. Blue circles represent ocean profiles while black squares represent land profiles. Error bars correspond to ± 1 standard deviation (from O'Dell and Bauer, 2007).

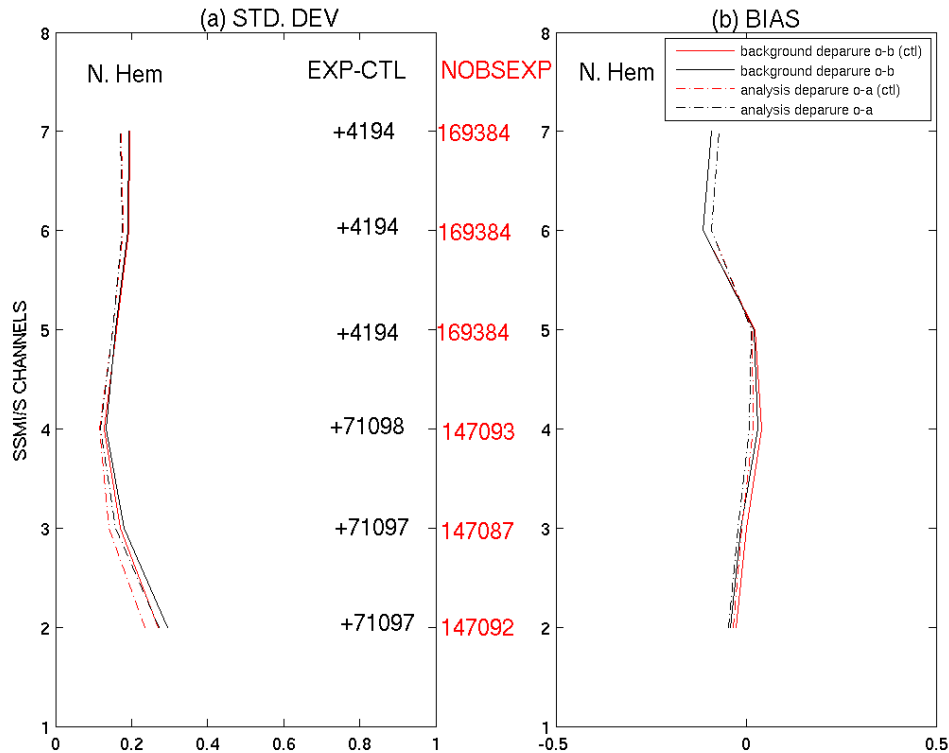


Fig. 6: Statistics for the First Guess (solid) and the analysis departures (dashed) for used SSMI/S observations for the experiment-dyn (black) and the control (red). Panels (a) and (b) show the standard deviations (K) and the bias (K) versus SSMI/S channels respectively. The number of used SSMI/S observations in experiment-dyn is also shown (in red) as well as the difference EXP-CTL given in black. (From Karbou *et al.* 2007).

GHz, 53.6 GHz and 54.4 GHz respectively) over land results in an increase of up to 93% in the number of used observations with respect to the SSMI/S control over the Northern Hemisphere for these channels. Many more data are assimilated over land when the surface emissivity is constrained by channel 1 (50GHz). Considering data over land only, the RMS errors of fg-departures for channels that receive a greater contribution from the surface (not assimilated but monitored) are much smaller for experiment-dyn and experiment-skin than for the SSMI/S control. The improvement of RMS error is very significant. The RMS error changes from nearly 7 K (control) to 2 K and from 11 K (control) to 2.5 K for channels 14 (22.2-V GHz) and 8 (150-V GHz) respectively. These results suggest that observations made at these frequency could potentially be assimilated over land. The forecast performances of the control experiment compared to our experiments indicate that there is a small positive impact on forecast of the geopotential height. This positive impact occurs over the Southern Hemisphere (for both experiment-dyn and experiment-skin) and the Northern Hemisphere (only for experiment-skin). Figure 7 shows the correlation between the 500 hPa geopotential height anomalies of the forecasts and the verifying analyses with the forecasts; the forecasts being verified against their own analyses for the whole assimilation period (32 forecasts). Results are given for experiment-skin (blue), the control experiment (red), the Northern Hemisphere (top) and the Southern Hemisphere (bottom). More SSMI/S experiment results can be found in Karbou *et al.* 2007.

A second set of experiments has been run using AMSU-A and AMSU-B observations. A control and another experiment (called experiment-dyn1) have been conducted. The experiments assimilate the same AMSU-A

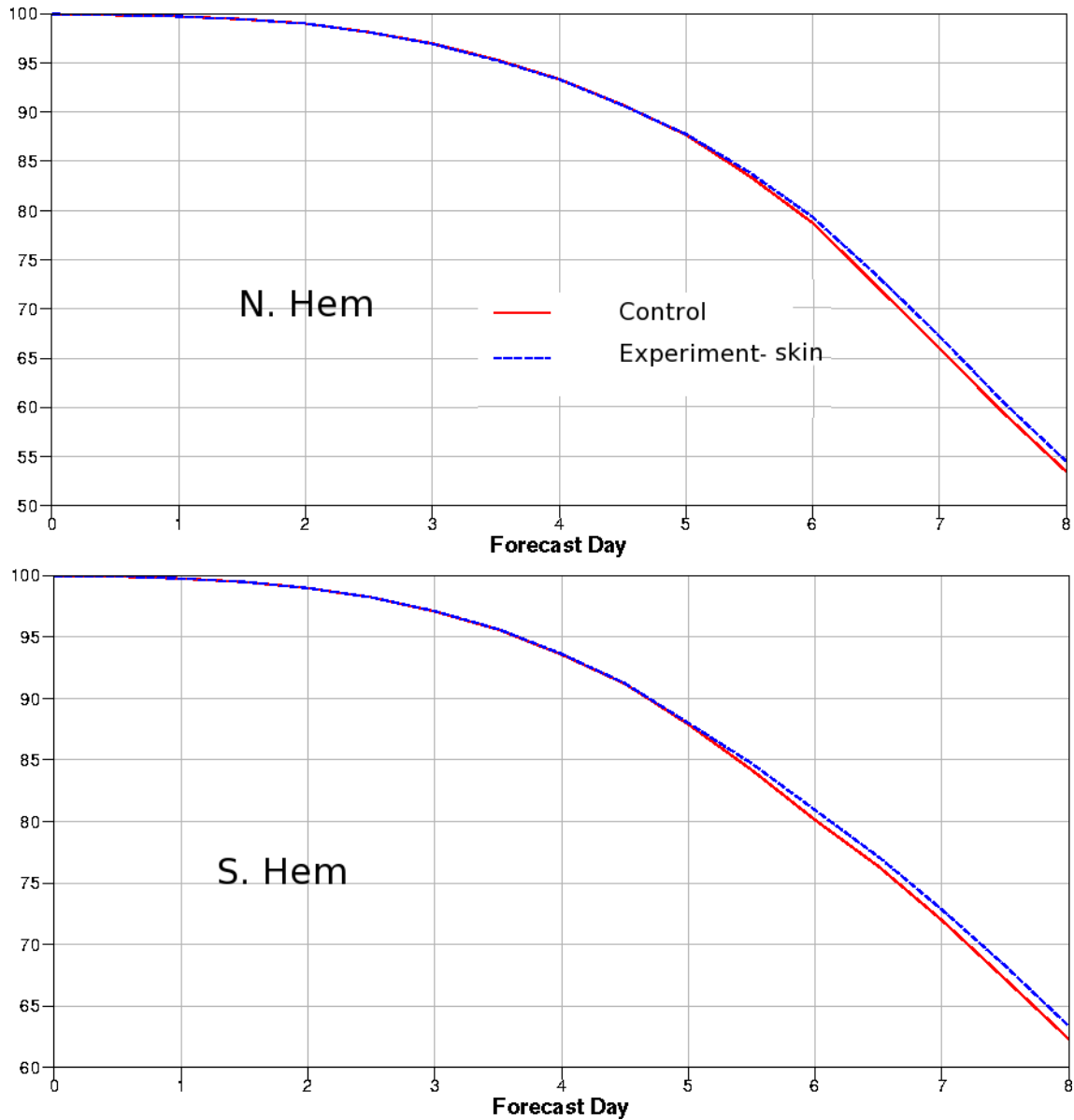


Fig. 7: Anomaly correlation for the 500 hPa geopotential height forecast with respect to the verifying analysis as a function of forecast range and for the Northern Hemisphere (top) and the Southern Hemisphere (bottom). Results are given for the experiment-skin that assimilates SSMI/S temperature channels over land and sea (blue curves) and for the control experiment. Scores have been calculated using the whole assimilation period (32 forecasts). (From Karbou et al. 2007).

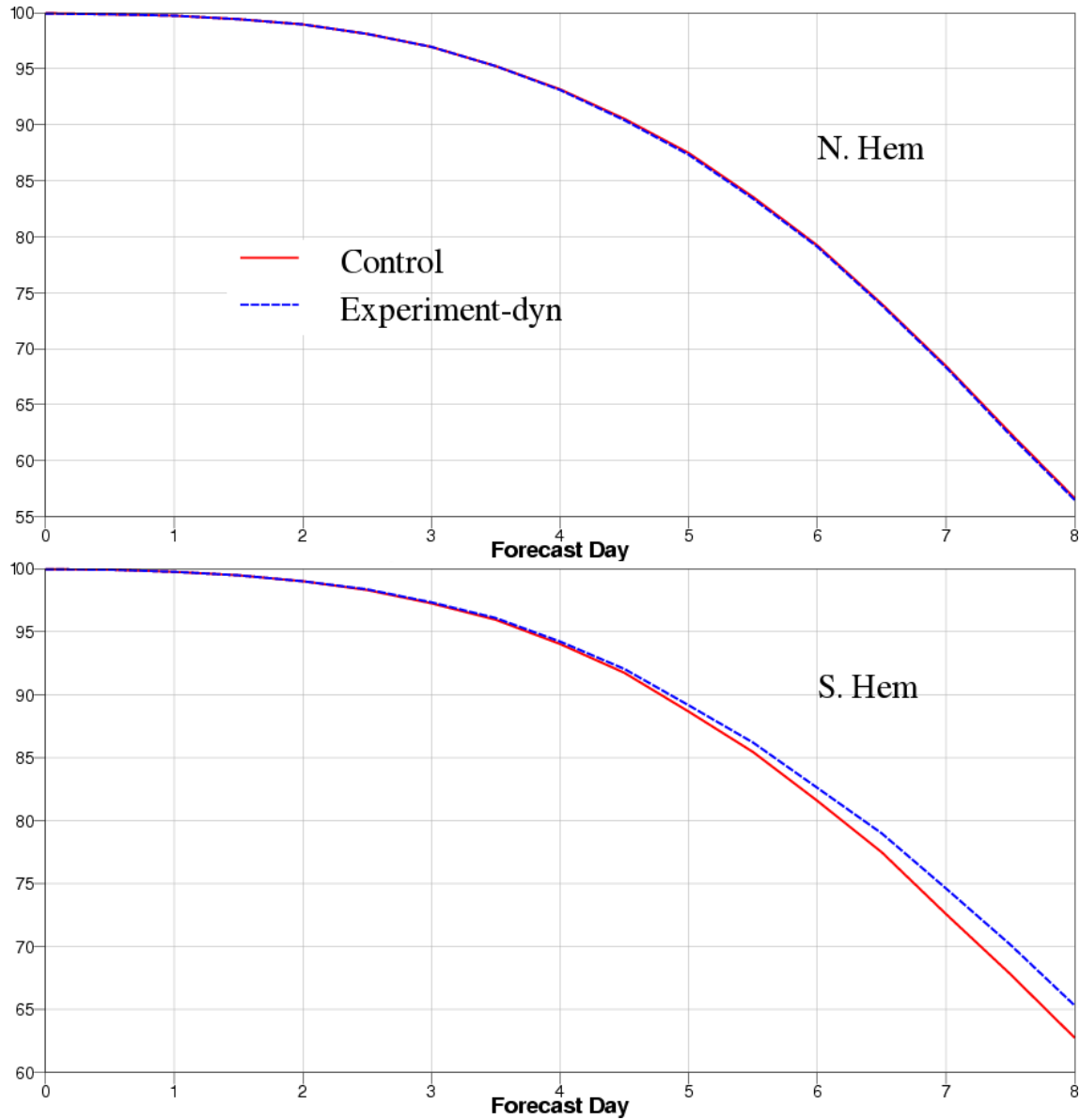


Fig. 8: Anomaly correlation for the 500 hPa geopotential height forecast with respect to the verifying analysis as a function of forecast range and for the Northern Hemisphere (top) and the Southern Hemisphere (bottom). Results are given for the experiment-dyn1 that assimilates AMSU-A temperature channels over land and sea (blue curves) and for the control experiment. Scores have been calculated using 62 forecasts.

and AMSU-B channels over land but use different schemes for the land emissivity: the model emissivity for the control and emissivities dynamically estimated from AMSU-A channel 2 (31.4 GHz) and from AMSU-B channel 1 (89 GHz). An increase of up to 18 % in the number of assimilated observations has been noted for AMSU-A channels 5, 6, 7 with experiment-dyn with respect to the control. Similar results have been obtained for AMSU-B channels with an increase of about 28 % for channel 3 AMSU-B. Note that the experiments use a check on the First Guess departures of the window channels 4 for AMSU-A (absolute departures should be below 0.7 K) and 2 for AMSU-B/MHS (absolute departures should be below 5.0 K) to identify data with a too strong cloud contamination for the lower-peaking channels. The updated emissivities in experiment-dyn will result in tighter histograms of FG departures as noted earlier, thus leading to more data considered cloud-free over land in this experiment. This also contributes to the larger number of observations assimilated in experiment-dyn. The forecast performances of the control experiment compared to the experiment-dyn indicate that positive impacts on forecast of the geopotential height and of the temperature occur over the Southern Hemisphere. The impacts are statistically significant (90% of confidence level) at levels ranging from 1000 hPa to 200 hPa. The impact over the Northern Hemisphere is almost neutral. Figure 8 shows the correlation between the 500 hPa geopotential height anomalies of the forecasts and the verifying analyses with the forecasts; the forecasts being verified against their own analyses for the whole assimilation period (62 forecasts). Results are given for experiment-dyn (blue), the control experiment (red), the Northern Hemisphere (top) and the Southern Hemisphere (bottom).

Other research studies are ongoing at ECMWF to complement the results obtained by Karbou *et al.* 2007. In particular, methods 2 and 3 (dynamic estimation of the land emissivity and the skin temperature respectively) are intensively tested within many assimilation experiment designs. It has been found that significant improvements in terms of forecast scores are obtained when the bias correction is improved over land.

Conclusions

Large uncertainties about the land surface emissivities and the skin temperatures are behind the still restricted use of microwave observations over land. These observations contain valuable information about the surface and the atmosphere and deserve to be assimilated in NWP models. Recent assimilation experiments have been conducted in order to assimilate more microwave observations over land. To do so, different methods have been used in order to estimate the land emissivity and/or the land skin temperature directly from satellite observations. Studies performed at the Met-Office, at MÉTÉO-FRANCE and at ECMWF have been described. In clear sky, three strategies, developed at MÉTÉO-FRANCE, have been found very promising in improving the assimilation of microwave observations over land. These methods have been tested within the constraints of the ECMWF assimilation system with similar findings. In cloudy situations, initial studies at ECMWF have shown that the assimilation of cloudy SSMI/S observations over land can be performed using carefully selected channels. These activities are pursued since more in depth studies are still needed to address the land affected observation assimilation issues. In particular, further developments to investigate the bias correction over land, the channels quality control and the effect of clouds should be of great interest.

The NWPSAF web site hosts a new page dedicated to infrared and microwave land emissivity estimation and modeling. The site contains links to many databases and models:

<http://www.metoffice.gov.uk/research/interproj/nwpsaf/rtm/emissivity/index.html>

Acknowledgements

The author would like to acknowledge contributions from Peter Bauer (ECMWF), Niels Bormann (ECMWF), John Derber (NCEP), Elisabeth Gérard (CNRM/GAME), Masahiro Kazumori (JMA/JCSDA), Blazej Krzeminski

(ECMWF), Christopher O'Dell (ECMWF), Florence Rabier (CNRM/GAME), Jean-Nol Thépaut (ECMWF), Sreerekha Thonipparambil (Met-Office), Paul van Delst (NOAA). The author would like to deeply thank François Bouttier, Jean-François Mahfouf and Florence Rabier for their suggestions and comments to improve the presentation associated with the manuscript. The author is also very grateful to Jean Maziejwski for his suggestions to improve the manuscript.

References

- Bauer, B. P. Lopez, A. Benedetti, D. Salmond and E., Moreau, 2006a: Implementation of 1D+4D-Var assimilation of precipitation-affected microwave radiances at ECMWF, Part I: 1D-Var. *Q. J. R. Meteorol. Soc.* **132**, 2277-2306.
- Bauer, B. P. Lopez, A. Benedetti, D. Salmond, S. Saarinen and M., Bonazzola, 2006b: Implementation of 1D+4D-Var assimilation of precipitation-affected microwave radiances at ECMWF, Part II: 4D-Var. *Q. J. R. Meteorol. Soc.* **132**, 2307-2332.
- Calvet, J. -C., J. P. Wigneron, A. Chanzy, S. Raju and L., Laguerre, 1995: Microwave dielectric proprieties of a silt-loam at high frequencies. *IEEE Trans. on Geoscience and Remote Sensing.* **33**, 634-642.
- Choudhury, B. J. , 1993 : Reflectivities of selected land surface types at 19 and 37 GHz from SSM/I observations. *Remote Sens. Environ.* **46**,1-17.
- Deblonde, G., and S. English ,2000: Evaluation of fastem and fastem2 fast microwave oceanic surface emissivity model. *Proceeding of the 11th International ATOVS study conference.* , Budapest, Hungary, 67-78
- English, S., 1999: Estimation of temperature and humidity profile information from microwave radiances over different surface types. *J. Applied Meteorology.* **38**, 1526-1541.
- English, S., 2007: The importance of accurate skin temperature in assimilating radiances from satellite sounding instruments. *IEEE Trans. On Geoscience and Remote sensin.* in press.
- Eyre, J. R., 1991: A fast radiative transfer model for satellite sounding systems. *ECMWF Tech. Memo.* **176**, 28 pp.
- Felde, G. W., and J. D. Pickle , 1995 : Retrieval of 91 and 150 GHz Earth surface emissivities. *J. Geophys. Res.* **100**, D10, 20,855-20,866.
- Grody, N. C. , 1988: Surface identification using satellite microwave radiometers. *IEEE Trans. On Geoscience and Remote sensing* **26**,850-859.
- Guillou, C., W. Ellison, L. Eymard, K. Lamkaouci, C. Prigent, G. Delbos, G. Balana, and S. A. Boukabara, 1998: Impact of new permittivity measurements on sea surface emissivity modelling in microwaves. *Radio Science* **33**, 649-667.
- Guissard, A., and P. Sobieski, 1987: An approximate model for the microwave brightness temperature of the sea. *Int. J. Remote Sens.* **8**, 1607-1627.
- Hewison, T. J., 2001: Airborne measurements of forest and agricultural land surface emissivity at millimetre wavelengths. *IEEE Trans. Geosci. Remote sensing.* **39**,2,393-400.
- Hewison, T. and S. English, 1999: Airborne retrieval of snow and ice surface emissivity at millimetre wavelengths. *IEEE Trans. Geosci. Remote sensing.* **37**,4, 1871-1879.
- Isaacs, R. G., Y. -Q. Jin, R. D. Worsham, G. Deblonde, and V. J. Falcone , 1989: The RADTRAN microwave surface emission models. *IEEE Trans. Geosci. Remote sensing* **27**,433-440.

- Jones, A. S., and T. H. Vonder Haar, 1997: Retrieval of microwave surface emittance over land using coincident microwave and infrared satellite measurements. *J. Geophys. Res.* **102**, D12, 13,609-13,626.
- Karbou, F., 2005: Two microwave land emissivity parameterizations suitable for AMSU observations. *IEEE Trans. on Geoscience and Remote Sensing.* **43**, 8, 1788-1795.
- Karbou, F. and C. Prigent, 2005: Calculation of microwave land surface emissivities from satellite observations: validity of the specular approximation over snow-free surfaces ? . *IEEE Trans. Geosci. Remote Sensing Letters.* **2**, 3, 311-314.
- Karbou, F., C. Prigent, L. Eymard and J. Pardo, 2005a: Microwave land emissivity calculations using AMSU-A and AMSU-B measurements. *IEEE Trans. on Geoscience and Remote Sensing.* **43**, 5, 948-959.
- Karbou, F., F. Aires, C. Prigent and L. Eymard, 2005b: Potential of Advanced Microwave Sounding Unit-A (AMSU-A) and AMSU-B measurements. for temperature and humidity sounding over land. *J. Geophysical Research.* **110**, D07109, doi:10.1029/2004JD005318.
- Karbou, F., E. Gérard and F. Rabier, 2006: Microwave Land Emissivity and Skin Temperature for AMSU-A and AMSU-B assimilation over land. *Q. J. R. Meteorol. Soc.* **132**, pp. 2333-2355
- Karbou, F., N. Bormann and J-N. Thépaut, 2007: Towards the assimilation of satellite microwave observations over land: feasibility studies using SSMI/S, AMSU-A and AMSU-B. *NWP-SAF Report*, 37 p.
- Kazumori, M., Q. Liu, R. Treadon, J. C. Derber, F. Weng, and S. J. Lord, 2007: Impact study of AMSR-E radiances in the NCEP global data assimilation system. *11th Symposium on Integrated Observing and Assimilation Systems for the Atmosphere, Oceans, and Land Surface (IOAS-AOLS)*
- Matricardi, M., F. Chevallier, G. Kelly, and J. N. Thépaut, 2004: An improved general fast radiative transfer model for the assimilation of radiance observations. *Q. J. R. Meteorol.* **130**, 153-173.
- Mätzler, C., 1990: Seasonal evolution of microwave radiation from an oat field. *Remote Sens. Environ.* **31**, 161-173.
- Mätzler, C., 1994: Passive microwave signatures of landscapes in winter. *Meteorol. Atmos. Phys.* **54**, 241-260.
- Mätzler, C., 2005: On the determination of surface emissivity from satellite observations, IEEE Geoscience and remote sensing letters., *IEEE Geosci. remote sensing letters.* **2**, 2, 160-163.
- Morland, J. C., David I. F. Grimes, G. Dugdale and T. J. Hewison, 2000: The Estimation of Land Surface Emissivities at 24 GHz to 157 GHz Using Remotely Sensed Aircraft Data. *Remote Sens. Environ.* **73**,3,323-336.
- Morland, J. C., David I. F. Grimes and T. J. Hewison, 2001: Satellite observations of the microwave emissivity of a semi-arid land surface. *Remote Sens. Environ.* **77**,2,149-164.
- Prigent, C., P. Abba, 1990: Sea surface equivalent brightness temperature at millimeter wavelength. *Annales Geophysicae* **8**, 627-634.
- Prigent, C., W. B. Rossow, and E. Matthews, 1997: Microwave land surface emissivities estimated from SSM/I observations. *J. Geophys. Res.* **102**, 21,867-21,890.
- Prigent, C., F. Chevallier, F. Karbou, P. Bauer and G. Kelly, 2005: AMSU-A surface emissivities for numerical weather prediction assimilation schemes. *J. Applied Meteorology.* **44**, 416-426.
- Prigent, C., F. Aires and W.B. Rossow, 2006: Land surface microwave emissivities for a decade. *Bull. Am. Meteor. Soc.* **87**, 1573-1584.
- O'Dell, C. and P. Bauer, 2007: Assimilation of precipitation-affected SSMI/S radiances over land in the ECMWF data assimilation system. *SAF-HYDRO Report*, 51p.

- Rosenkranz, P. W. and D. H. Staelin, 1972: Microwave emissivity of ocean foam and its effect on nadiral radiometric measurements. *J. Geophys. Res.* **77**, 6528-6538.
- Saunders, R. W., M. Matricardi, and P. Brunel, 1999: An improved fast radiative transfer model for assimilation of satellite radiance observations. *Quart. J. Roy. Meteor. Soc.* **125**, 1407-1425.
- Weng, F., B., Yan, and N. Grody, 2001: A microwave land emissivity model. *J. Geophys. Res.* **106**, D17, 20,115-20,123.
- Wentz, F., 1975: A two scale scattering model for foam-free sea microwave brightness temperatures. *J. Geophys. Res.* **80**, 3441-3446.
- Wigneron, J. -P., D. Guyon, J. -C. Calvet, G. Courrier, and N. Bruignier, 1997: Monitoring coniferous forest characteristics using a multifrequency microwave radiometry. *Remote Sens. Environ.* **60**, 299-310.